

Simulation of the formation of nonequilibrium structures in magnetorheological fluids subject to an external magnetic field

M. Mohebi and N. Jamasbi

Center for Scientific Investigation and Higher Education of Ensenada, Ensenada, Baja California, Mexico

Jing Liu

California State University, Long Beach, California 90840

(Received 16 February 1996)

We developed a computer model to understand the nonequilibrium structures induced in a magnetorheological (MR) fluid by rapidly applying an external magnetic field. MR fluids consist of particles suspended in a liquid where particles interact through dipole moments induced by the external magnetic field. We have simulated these induced structures in both directions, parallel and perpendicular to the field, in the limit of fastest response, by neglecting thermal motion and applying the field instantaneously. Our results show that the process of structure formation starts with particles forming chains aligned with the external field. The chains then coalesce to form columns and wall-like structures ("worms" as viewed from the top). The complexity of this pattern is found to depend on the concentration of particles and the confinement of the cell in the direction of the external field. These results are consistent with experimental observations [G.A. Flores *et al.*, in *Proceedings of the Fifth International Conference on ER Fluids, MR Suspensions, and Associated Technology*, University of Sheffield, Sheffield, July 1995, edited by W. Bullough (World Scientific, Singapore, 1996), p. 140]. We have also used this model to study the interaction of two chains. The results of this study help in the understanding of the connection between the thickness of the sample and the increased complexity of the observed lateral pattern. [S1063-651X(96)09011-3]

PACS number(s): 83.80.Gv, 61.20.Ja, 61.90.+d, 82.70.Dd

INTRODUCTION

Magnetorheological (MR) fluids, in general, consist of micrometer-size particles such as iron oxide suspended in a host medium such as water or oil [1–3]. Without an external magnetic field, these particles have no permanent dipole moments and therefore are in Brownian motion. Application of an external magnetic field induces a magnetic dipole moment in each particle. Thus the particles interact through the induced magnetic dipole moments. Depending on their positions, they can attract or repel one another. As a result of this interaction, a structure is formed that eventually freezes in space, as the applied magnetic field increases. This system is similar to electrorheological (ER) fluids, where an electric dipole moment is induced in each dielectric particle suspended in a liquid by application of an external electric field [4–7]. The dramatic increase and reversibility of the viscosity of the ER and MR fluids with the application of the external field has made these systems of great potential for industrial applications [8–10].

Experimental research in the study of the field-induced structures in the ER and MR fluids so far have been mostly limited to the case of equilibrium state, where the external field is applied slowly [2,3,11–13]. In these studies, for the case of a rapidly increasing field [14], the cell thickness is either very small or extremely large, as in the case of ER fluids [15,16]. Most simulation studies reported in the literature, on the other hand, have been performed for the ER fluids, where a periodic boundary condition is applied in all directions [17–20]. This boundary condition is consistent

with the ER fluid experiments because conducting boundaries are used. Due to image charges, chain lengths are equivalently infinite. In MR fluid experiments where coils are used to apply the magnetic field and the sample is confined by nonferrous materials (glass), image dipoles analogous to those in ER fluids do not exist. Therefore, a finite boundary in the direction of the applied field is present and one can study the effect of cell confinement on the structures formed. While many researchers have done valuable work in simulating structure formations in ER fluids [17–20], including effects of thermal motion and hydrodynamic interactions, and have identified many of the structural features of these materials, a simulation with a different boundary condition is required for MR fluids that are not bounded by high permeability materials.

When the field is applied slowly, the thermal motion of the particles allows the particles to find their lowest-energy configuration, which is a system of chains and columns (multiple chains attached in parallel) [3,5,15]. In this case the thermal motion plays a significant role in the structure formation and must be included in the model. However, when the field is applied rapidly the magnetic interaction of the particles dominates their random thermal motion. Under these conditions, as observed in experiments with ferrofluid emulsions [1], particles quickly interlock into a complex labyrinthine structure with complexity depending on the boundary condition and sample concentration. This nonequilibrium structure, induced with the fast application of the field has received little attention both experimentally and theoretically.

We have undertaken this study in an attempt to understand these experimentally observed complex structures. Here we report the results of computer simulation of MR fluids when the external field is applied instantaneously. Our model is in qualitative agreement with the experimental observations. First, there are two distinct time scales: a fast one for the formation of chains and a slower one for the formation of labyrinthine structure. Second, we confirm a direct correlation between the sample thickness and the complexity of the pattern as observed in the direction of the applied field.

Furthermore, the simple model used here reveals that the chain-chain interaction depends sensitively on the relative shift along the chain direction. The attractive-interaction range for chain coarsening depends on the chain length, which explains the dependence of structure complexity on cell thickness and particle volume fraction. One of the advantages of using MR fluids with nonmagnetic boundaries over ER fluids is the flexibility in changing the chain length by varying sample cell thickness. Although similar labyrinthine structures have been observed in ER fluids [11], to our knowledge these structures have not been the focus of any theoretical study so far.

MODEL

To compare with the experimental results, we consider a monodisperse suspension of spherical particles in water. All the particles have a radius a , with a magnetic permeability $\mu = \mu_0(1 + \chi)$, where χ is the magnetic susceptibility of the particles. When there is no external magnetic field, the particles are randomly distributed throughout the volume. Application of a uniform external magnetic field \mathbf{B}_e induces a magnetic moment in each particle. As in other simulations [17–20], we consider the dipole approximation.

If we ignore the magnetic susceptibility of water, the induced dipole moment is $\mathbf{m} = (4\pi a^3/\mu_0)[(\mu - \mu_0)/(\mu + 2\mu_0)]\mathbf{B}_e$ (mks), which is in the same direction as the applied field, i.e., the direction of the z axis. This means that the force acting on each particle due to the external field is zero. However, there is a force acting on each particle as a result of the sum of the magnetic fields of all the other particles in the surrounding liquid. The three components of the force of particle i on particle j are given in

$$\begin{aligned} F_{x,ij} &= -\frac{3Qx_{ij}}{r_{ij}^5} \left[\frac{5z_{ij}^2}{r_{ij}^2} - 1 \right], \\ F_{y,ij} &= -\frac{3Qy_{ij}}{r_{ij}^5} \left[\frac{5z_{ij}^2}{r_{ij}^2} - 1 \right], \\ F_{z,ij} &= -\frac{3Qz_{ij}}{r_{ij}^5} \left[\frac{5z_{ij}^2}{r_{ij}^2} - 3 \right], \end{aligned} \quad (1)$$

where $x_{ij} = x_i - x_j$, $y_{ij} = y_i - y_j$, $z_{ij} = z_i - z_j$, $r_{ij} = \sqrt{x_{ij}^2 + y_{ij}^2 + z_{ij}^2}$, and $Q = (4\pi a^6/\mu_0)[\chi/(\chi + 3)]^2 B_e^2$. Here we have also ignored the effect of the dipole field of the surrounding particles on the induced dipole moment. This

approximation is valid for low external fields, which is the case in experiments ($B \leq 400$ G). The equation of motion for the i th particles is

$$m \frac{d^2 \mathbf{r}_i}{dt^2} + D \frac{d\mathbf{r}_i}{dt} = \mathbf{F}_i, \quad (2)$$

where m is the mass of each particle, \mathbf{r}_i is the position vector of the i th particle, $\mathbf{F}_i = \sum_j \mathbf{F}_{ij} + \mathbf{F}_i^r$ is the total force acting on the i th particle, and $D = 6\pi a\eta$ is the Stokes drag coefficient for a solid sphere, of radius a , moving in a liquid with viscosity η .

In the expression for the force, $\mathbf{F}_i^r = \mathbf{F}_{i(\text{wall})}^r + \mathbf{F}_{i(\text{hard sphere})}^r$ is a strong repulsive force with two components, which we have introduced to account for the effect of the walls of the container and the hard spherical particles. If we consider a volume with the size of L_x , L_y , and L_z , the repulsive force of the walls are calculated from

$$\mathbf{F}_{i(\text{wall})}^r = \frac{3QB^2}{8a^4} [e^{-40(z_i/a-1)} + e^{-40[(L_z-z_i)/a-1]}]. \quad (3)$$

In the experiments, the field is applied in the z direction to a cell thickness of L_z . There are no walls in the x and y directions; therefore, in these directions a periodic boundary condition is used. This repulsive force rapidly drops to zero as a particle is moved away from the walls and it increases exponentially if its surface penetrates into the wall. The second component in \mathbf{F}_i^r is a similar repulsive force between all the particles to simulate a hard-sphere interaction between them when in contact. This force is calculated from

$$\mathbf{F}_{i(\text{hard sphere})}^r = \sum_j \left[\frac{3QB^2}{8a^4} e^{-40(r_{ij}/2a-1)} \right]. \quad (4)$$

Since we are interested in the rapid application of the field, we have ignored the random Brownian motion of the particles. This is because the magnetic energy (W_m) quickly dominates the thermal energy (KT) of the particles, which corresponds to a coupling constant [1–3] $\lambda = W_m/KT \gg 1$. It has been suggested by Halsey and Toor [22] that even when the interaction strength is large, the Brownian motion can play a significant role in structure formation. This effect is not directly because of thermal rearrangement of individual particles, but because of the modification of the long-range chain-chain interaction. According to Ref. [22], this fluctuation-induced long-range interaction is important when chain separation is of the order of the fluctuation wavelength in the chains. The lowest-energy fluctuation wavelength is equal to the chain length. Then, given the same chain length in a dilute sample, where the chain separation is larger, this effect is more significant compared to a concentrated sample where the chain separation is much smaller than the chain length. We have previously used Halsey and Toor's theory successfully to explain our experimental data with 3% volume fraction [21,23]. In this work, however, we are simulating a volume fraction of 10%, where the chain separation is smaller. Therefore, the effect of the direct dipolar interaction is more significant than the thermally induced fluctuations in chains.

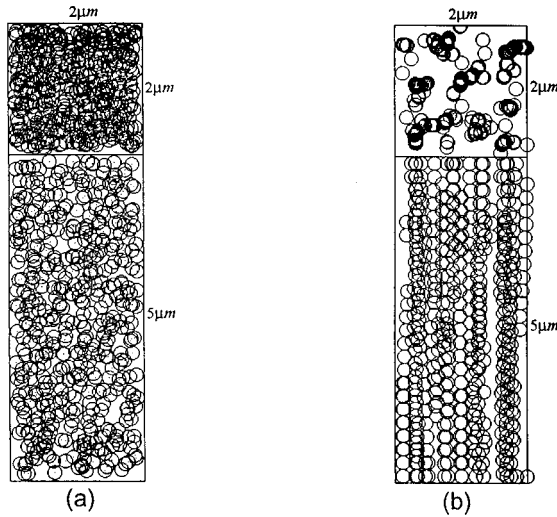


FIG. 1. Top and side views of a $2 \times 2 \times 5 \mu\text{m}^3$ volume. The dimensions are given in micrometers. There are 478 particles. The volume fraction is 0.1. The particle size is $0.2 \mu\text{m}$. (a) Initially particles are randomly positioned. (b) 14 ms after the application of the external magnetic field (400 G) the structure has been formed.

We can integrate Eq. (2) exactly for a short-time interval τ by assuming that this time step is short enough so that the force \mathbf{F}_i remains constant for all particles. The change in the position vector of the i th particle is then given by

$$\Delta \mathbf{r}_i = \frac{\mathbf{F}_i}{D} \tau + \frac{m}{D} \left(\frac{\mathbf{F}_i}{D} - \mathbf{V}_{0i} \right) e^{-D\tau/m}. \quad (5)$$

Here V_{0i} is the velocity of the i th particle at the beginning of the time interval τ . The final velocity of the particle at the end of the time interval τ can be found from

$$\mathbf{V}_{\tau i} = \frac{\mathbf{F}_i}{D} + \left(\mathbf{V}_{0i} - \frac{\mathbf{F}_i}{D} \right) e^{-D\tau/m}. \quad (6)$$

We now proceed to calculate the new position of all the particles in a stepwise manner by using the final velocity $\mathbf{V}_{\tau i}$ as the initial velocity in the next time step. Note that \mathbf{F}_i/D is the terminal velocity of the particle and that the exponential terms in Eqs. (5) and (6), which represent the effect of acceleration, quickly vanish with time. Therefore, the effect of acceleration can be ignored for time steps of the order of microseconds, since $m/D \approx 10^{-8}$ s. Thus, instead of using Eq. (5), we can calculate the new position of the particle from

$$\Delta \mathbf{r}_i = \frac{\mathbf{F}_i}{D} \tau. \quad (7)$$

We start by placing particles in the volume at random positions. At $t=0$ the magnetic field is turned on. The new position for all the particles is calculated after the time interval of τ . This time interval is automatically adjusted to ensure optimum simulation time. The process is repeated until the magnitude of the displacement vector for all the particles is less than a predetermined value.

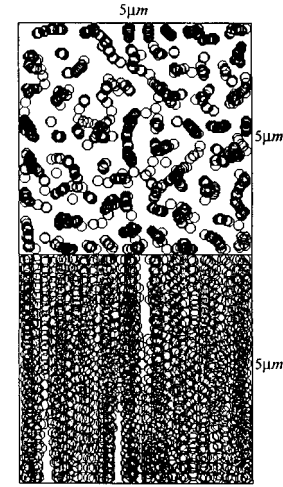


FIG. 2. The labyrinthine pattern is more apparent when a larger cross section is viewed. Here the simulated volume is $5 \times 5 \times 5 \mu\text{m}^3$. The dimensions are given in micrometers. The particle size and volume fraction are the same as in Fig. 1. An external magnetic field of 400 G is applied instantaneously.

RESULTS

Initially the particles are placed in the volume at random positions. Figure 1(a) shows the top and side views of a volume of $2 \times 2 \times 5 \mu\text{m}^3$ at $t=0$, before the application of the field. In this simulation volume there are a total of 478 spherical particles with a diameter of $0.2 \mu\text{m}$ each. This corresponds to a volume fraction of $\phi=0.1$. Figure 1(b) shows the top and side views of the same simulation at $t=14$ ms. After a magnetic field of 400 G ($\lambda=36$) is applied instantaneously, the particles attract or repel one another depending on their positions. Small chains are formed quickly, aligned with the applied magnetic field. In less than 2 ms these small chains are connected and longer chains are formed. The chains may then attract or repel one another depending on their lengths, separations, and relative vertical positions. This process is much slower and may take from several tens of milliseconds to 1 s, depending on the thickness of the cell. Eventually, a steady state is reached and a complex pattern is formed, which can be viewed in the direction of the field, as shown in Fig. 1(b).

When the field is applied rapidly in a thin cell ($L_z \sim 20a$), after reaching steady state, single separated chains are observed in a nearly hexagonal lattice. As the cell thickness is increased separate columns are observed. For thicker samples, however, more complex patterns can be observed in the lateral direction. In such a case the chains form vertical sheets that are generally curved and branched. Viewed in the direction of the field, they appear labyrinthine, as shown in Fig. 2. For a given volume fraction the complexity increases as the thickness of the sample (chain length) increases. The same behavior is observed when the volume fraction is increased. This is consistent with the experimental observations [1].

In order to characterize the complexity of the observed pattern, we define two parameters: the vertical connectivity (C_V) and the horizontal connectivity (C_H). Here connectivity is defined as the ratio of the total number of contact

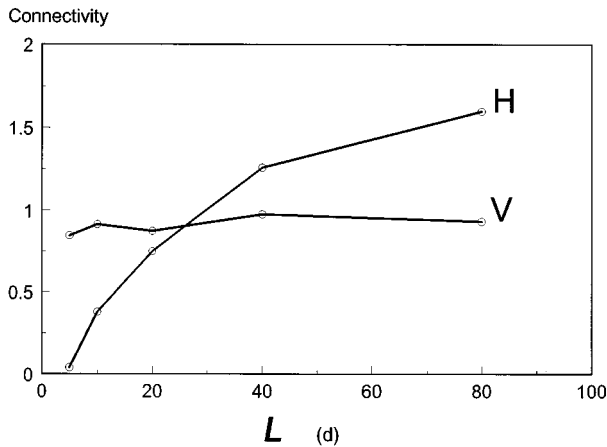


FIG. 3. Unitless horizontal and vertical connectivities plotted versus the thickness of the cell in units of particle diameter. The particle size and volume fraction are the same as in Fig. 1. An external magnetic field of 400 G is applied instantaneously.

points among all the particles divided by the number of particles minus one, which is a statistical average of the number of contact points per particle. Two particles are considered to be in contact if their gap is less than 5% of their diameter. Two particles are considered to be in vertical contact if the center to center line is within 30° on either side from the vertical direction and they are considered to be in horizontal contact if the center to center line is within 60° on either side from the horizontal plane.

The value of C_V reflects the degree to which chains have formed. For example, if all particles form one vertical chain we would have $C_V=1$, which is the maximum value it can have, and in this case $C_H=0$. The value of C_H reflects the complexity of the structure in the lateral direction. Since in this direction a particle can make contact with more than two other particles, the maximum value of C_H can be greater than one. For example, for a two-dimensional lattice of hexagonal-close-packed sheet of particles in a horizontal plane, we would have $C_H=3$ and $C_V=0$.

Figure 3 shows the calculated C_V and C_H , from our simulation, as a function of sample thickness in the direction of the applied field. Here an area of $1 \times 1 \mu\text{m}^2$ in the lateral direction is considered, with the cell thickness changing from 1 to $16 \mu\text{m}$. The particle size is $0.2 \mu\text{m}$ and $\phi=0.1$ for all calculations. We can see that C_V is essentially constant. This means that the formation of chains is independent of the thickness of the cell. In all cases C_V reaches 0.97 in less than 2 ms. This also suggests that the time scale for the formation of chains is independent of the cell thickness. This is not the case, however, for the structure in the lateral direction. As the cell thickness is increased the lateral complexity increases. Furthermore, it takes a much longer time for the structure to form. In other words, saturation time increases with the cell thickness and it is several tens of milliseconds for the range of cell thicknesses considered here. This is consistent with experimental measurement [21] done at $\phi=0.03$.

In order to understand the relation between the cell thickness and the lateral complexity of the observed patterns, we first consider the simplest case: the interaction of two chains.

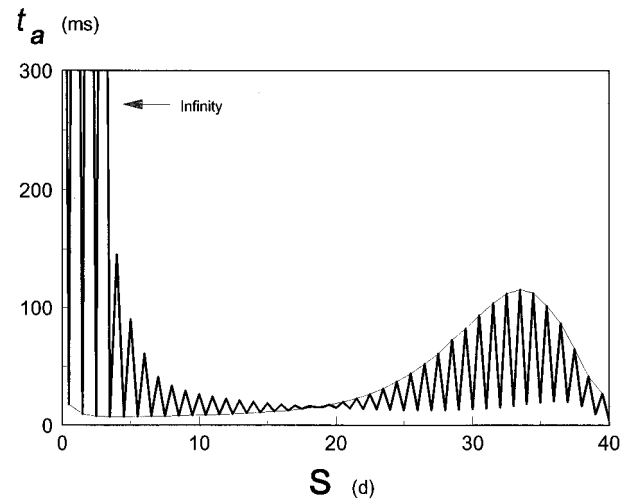


FIG. 4. Complete attachment time (t_a) of two parallel chains in milliseconds versus their relative vertical shift (S) in units of particle diameter. The chains are 40 particles long. The particle diameter is $0.2 \mu\text{m}$. An external magnetic field of 400 G is applied instantaneously. Infinite time means that the chains repel one another. The fine line in this figure connects all the points that correspond to the off-registered initial positions.

Two parallel chains of equal length with no vertical shift repel one another, independent of their lengths. Obviously, in this case it is not possible for chains to coalesce and form any aggregates. For two infinitely long chains with a relative shift of an odd number of particle radius (which are called-off registered positions), the interaction between two straight chains is short ranged but attractive [7]. They will aggregate to form body-centered-tetragonal lattice as in the case of ER fluids [6]. However, for two parallel chains with finite chain lengths in an off-registered position, they may either attract or repel one another depending on the length of the chain, relative shift, and their horizontal separation. This is because of the existence of the additional repulsion between monopoles at the ends of the chains. The shorter the chain lengths, the more important the repulsive force at their ends. Therefore, for MR fluids in confined geometry without permeable boundaries, the structures formed are different from that observed in ER fluids. Instead of one aggregation, they are separated when chains are short (ten or fewer particles per chain) and separated columns for longer length where the column width increases with the chain length [3]. The repulsive force between monopoles at the ends of columns balance the attractive force between the rest of the chains. When permeable boundaries are used, the effective chain length goes to infinity. Separated phases of solid and liquid will be formed as in the case of ER fluids.

In the rest of the paper, we will concentrate on two-chain aggregation with finite chain length, which is a region that is not yet fully understood. We found that when the interaction of two chains is attractive, they first bend from the middle. They then make contact from the middle and the attachment propagates along the length of the two chains, towards both ends of the chains. This motion is similar to the way two sides of a zipper attach to one another. Although observed in experiments, attachment patterns for two chains in a helical form was never observed in our simulation.

Figure 4 is a plot of the time for the complete attachment of two chains (t_a), as a function of their relative vertical shift (S), which is changed from zero to the full length of each chain. Both chains are 40 particles long where the particle diameter is $0.2 \mu\text{m}$. Initially the two straight chains are placed in a large volume (no confinement) at a separation (r) of $0.34 \mu\text{m}$ and at a shift S . No other particle is present and the periodic boundary condition in the model is turned off. At time $t=0$ the magnetic field is turned on and the movement of the particles is followed until the attachment is complete. Notice that in this calculation both chains are free to bend as a result of their interaction. A short attachment time indicates a stronger attractive force and a long attachment time indicates a weaker attractive force between the two chains, while a repulsive interaction between two chains results in an infinite attachment time. The most striking feature of the curve in Fig. 4 is the oscillations in attachment time as S increases. Similar peaks may be expected to exist in the potential energy of the two chains as a function of S . All the peaks in the first half of the curve correspond to an S that is an even number of particle radius (a). This is when the centers of the particles in both chains are on the same horizontal plane. We call this a registered position for the two chains. All the valleys in the first half of the curve correspond to an S that is an odd number of a . These are called off-registered positions. In an off-registered position at $t=0$, two chains attract one another strongly at this given initial separation. A typical attachment time of 10–20 ms is observed. In registered positions at $t=0$, however, two chains repel one another. They may never get together, as the first four infinite peaks in Fig. 4 show. On the other hand, as S increases each chain experiences a net force along the chain direction, which slides them into an off-registered position. Then they attract each other as displayed by the peaks at $S=5-20$ in Fig. 4.

In the second half of the curve in Fig. 4 we find a very interesting and unexpected result. When the two chains are initially at an off-registered position there is a weaker attractive interaction shown as peaks. The stronger attractive interaction corresponds to the registered positions. This is shown by the thin line, which connects only the points that correspond to the off-registered initial positions. For $S < L/2$ all the minimas in the attachment time correspond to the off-registered positions. However, as the fine line in Fig. 4 shows, for $S > L/2$ the off-registered positions correspond to the maxima in the attachment time. This means that for $S > L/2$ two chains experience a stronger attractive force compared to the off-registered positions. This is in spite of the fact that in registered positions, particles in two chains initially repel one another. At first, this result seems against our intuition. We can understand it, however, from the following discussion.

When two chains are initially in an off-registered position, they experience a force with two components: a lateral attraction and a vertical sliding. With $S > L/2$, the vertical sliding force is stronger than the case of $S < L/2$. Furthermore, the direction of the sliding force alternates if the two chains move from one off-registered position to the next registered position. In the case where the initial position is off registered, the two chains start at the bottom of a valley in the lateral direction of their potential curve. As the chains

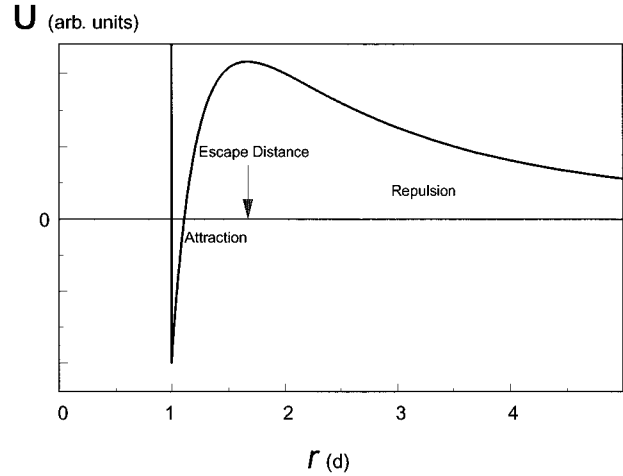


FIG. 5. Qualitative form of the interaction potential (U) of two parallel chains in arbitrary units, as a function of their distance (r) in units of particle diameter.

slide vertically in the direction of decreasing S , they move out of the lateral attractive valley in their potential curve, approaching a registered position. In order to get attracted they must go over one peak in the potential curve to fall into the next attractive valley (next off-registered position). The system must go over one hill to fall into the next valley. This process takes longer time. This happens when the sliding force is large, which is the case with $S > L/2$. Indeed, in this case final attached positions have a relative shift which is reduced by one particle. On the other hand, when two chains are initially in registered positions, they experience an initial sliding force and a lateral repulsive force. As they slide away from one another in the direction of increasing S , they arrive at an off-registered position. Their lateral repulsive component turns into a strong attractive force. In this case the two chains start at the top of a peak in their potential curve and fall directly to the first valley when they attach. This takes less time.

When the two chains are shifted vertically by their entire lengths, once attached, they form a single chain, 80 particles long, which gives the shortest attachment time. We can also see from Fig. 4 that around $S=L/2$ the attachment time is short and insensitive to the variations of S , indicating a strong attractive force. The strongest attractive interaction corresponds to $S \leq 10$ only at off-registered positions. This explains the conical shapes at both ends of each column observed in experiments [2,3]. In summary, at this initial horizontal separation $r=0.34 \mu\text{m}$, the two chains basically attract each other, except at a few positions where their initial relative vertical shift is small and the chains are in registered positions.

However, even at off-registered positions where the two chains are attracted at close range, there is a distance beyond which the interaction force becomes repulsive. If we now keep the vertical shift constant and increase their horizontal separation, they will reach a distance where the attraction turns into repulsion. We call this separation the escape distance (r_e). This result suggests that in addition to many peaks and valleys in the vertical direction, the interaction potential of two chains must have a maximum, at the escape

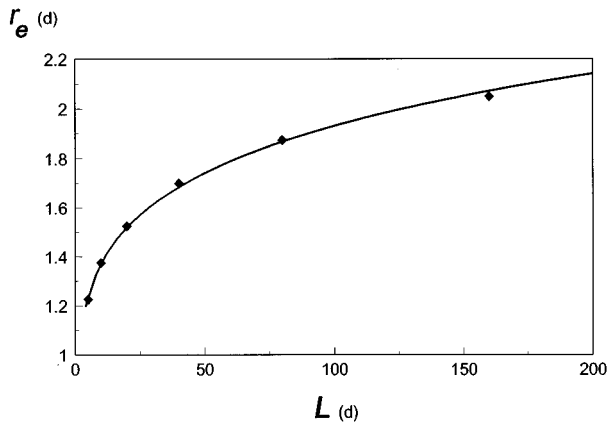


FIG. 6. Distance beyond which two chains repel (r_e , escape distance), plotted versus chain length (L), both in units of particle diameter. The vertical shift (S) in this case is equal to one particle radius for all the points. Under the curve, two chains attract; above the curve they repel one another. The particle diameter is $0.2 \mu\text{m}$. An external magnetic field of 400 G is applied instantaneously.

distance, in the lateral direction. There is also a minimum where the two chains are in contact. We can imagine that the interaction potential between two chains, as a function of their separation, has the qualitative form shown in Fig. 5. The infinite potential at $r=2a$ in Fig. 5 is due to the hard-sphere interaction between particles. The exact shape of this interaction potential depends on the length of the two chains and the amount of their relative vertical shift.

Figure 6 shows the dependence of the escape distance on the chain length, obtained from the simulation of two chains. The vertical shift in this case is constant at one particle radius, corresponding to an off-registered position. From the data we can see that the escape distance increases with the chain length. If the average distance between chains is greater than the escape distance, fewer chains coalesce and the resulting pattern is basically separated chains. If we reduce chain separation to within escape distance, by increasing volume fraction, more chains attract each other and separated aggregations form. This is what is observed in experiments [1].

The same behavior in structure formation is observed as the cell thickness increases. For a given volume fraction, the average chain separation is fixed and is independent of chain length. Thin cells allow only short chains to form and thicker cells allow longer chains to form. Since the escape distance increases with chain length, short chains repel each other and form separated single chains. Long chains attract one another and aggregate. For example, with a volume fraction of 0.1, the average chain separation is $r_{av} \sim a/\sqrt{\phi} = 1.58 \times 2a$. From Fig. 6, this means that chains with lengths less than 25 particles in diameter would repel each other and form separate chains. Longer chains attract one another and form aggregates. The longer the chains, the larger the aggregates. This also explains what is observed in the experiments [3,4] when the field is applied slowly: the diameter of the columns increases with the cell thickness. The shape of aggregation depends on how fast the chains approach each other during the aggregation process.

In this work we also found, in agreement with the experi-

mental observations [1], that the aggregation complexity of the lateral structure increases with the thickness of the cell. This arises from the fact that the chain-chain interaction potential has a maximum as shown in Fig. 5. For a given vertical shift, we showed that longer chains begin to attract one another at a greater distance, as they approach each other from far away. In a system where there are multitudes of chains of random length, position, and relative vertical shift, the total potential energy of the system can easily be imagined to have many local minima and maxima. When the field is applied rapidly, the system may get trapped in one of the local minima, which quickly becomes deep enough so that it cannot be overcome by the thermal energy of the particles. Since chains approach one another from random positions, they stick to one another (being trapped in local minima) also from random angles. Therefore, the observed labyrinthine pattern results from this equilibrium aggregation process. The longer the chains, the more chains are within the escape distance that attract each other. Thus more possible angles or ways exist for the chains to approach the aggregation center. A larger and more complex pattern is therefore produced. On the other hand, with slow ramping up of the applied field, the potential energy grows gradually. The thermal motion of the particles will have a chance to kick the system out of the local minima before they develop into big barriers. A global energy minimum thus can be reached that results in the experimentally observed columnar structures [2,3].

SUMMARY

We have developed a computer model to understand the nonequilibrium structures induced in a magnetorheological fluid by an external magnetic field. Our model clearly shows that there are two distinct time scales for the structure formation in the vertical and horizontal direction. By neglecting thermal motion and applying the field instantaneously, however, we obtain only the limit of fastest response to the applied magnetic field. In this limit, our simulations show that chains are formed within 2 ms. Our study indicates that this time is independent of the cell thickness. The time scale for the aggregation of chains, however, can be up to three orders of magnitudes longer. This is the time it takes for the particles to interlock in a motionless state. Our study confirms the direct dependence of this time on the cell thickness, as seen in experiments [1]. Our simulations of the interaction of two chains shows the importance of chain length and relative vertical shift in determining the attachment time and interaction range between chains during coarsening. From this we begin to understand the dependence of complexity of the nonequilibrium structure on the cell thickness.

ACKNOWLEDGMENTS

We thank George A. Flores from CSULB for his experiments that stimulated this simulation. We also thank Dr. Yun Zhu, Dr. Mark Gross, and Brandon Murakami for helpful discussions and Miguel Garcia for his assistance with the development of the computer code. One of us (J.L.) gratefully acknowledges the support by NASA, Grant No. NAG 3-1634, by NSF DMR, Grant No. 9321201, and by CSULB University Research and Academic Affairs Office.

- [1] G.A. Flores, M. L. Ivey, J. Liu, M. Mohebi, and N. Jamasbi, in *Proceedings of the Fifth International Conference on ER Fluids, MR Suspensions, and Associated Technology, University of Sheffield, Sheffield, July 1995*, edited by W. Bullough (World Scientific, Singapore, 1996), p. 140.
- [2] Jing Liu, E. M. Lawrence, M. L. Ivey, G. A. Flores, J. Bibette, and J. Richard, in *Proceedings of the Fourth International Conference on ER Fluids, Feldkirch, 1993*, edited by R. Tao, (World Scientific, Singapore, 1994), pp. 19–24.
- [3] Jing Liu, E. M. Lawrence, A. Wu, M. L. Ivey, G. A. Flores, K. A. Javier, J. Bibett, and J. Richard, *Phys. Rev. Lett.* **74**, 2828 (1995).
- [4] A. P. Gast and C. F. Zukoski, *Adv. Colloid Interface Sci.* **30**, 153 (1989).
- [5] T. C. Halsey and W. Toor, *Phys. Rev. Lett.* **65**, 2820 (1990).
- [6] R. Chen, R. N. Zitter, and R. Tao, *Phys. Rev. Lett.* **68**, 2555 (1992).
- [7] R. Tao and J. M. Sun, *Phys. Rev. Lett.* **67**, 398 (1991).
- [8] *Electromagnetic Fluids*, edited by J. P. Carlson, A. F. Sprecher, and H. Conrad (Technomic, Lancaster, PA, 1990).
- [9] J. E. Stangroom, *Phys. Technol.* **14**, 290 (1983).
- [10] *Proceedings of the Fifth International Conference on ER Fluids, MR Suspensions, and Associated Technology* (Ref. [1]).
- [11] E. Lemaire, Y. Grasselli, and G. Bossis, *J. Phys. (France) II* **2**, 359 (1992).
- [12] E. Lemaire, G. Bossis, and Y. Grasselli, *J. Phys. (France) II* **4**, 253 (1994).
- [13] M. Fermigier and A. P. Gast, *J. Colloid Interface Sci.* **54**, 522 (1992).
- [14] Y. H. Hwang and X. L. Wu, *Phys. Rev. E* **49**, 3102 (1994).
- [15] J. E. Martin, J. Odinek, and T. C. Halsey, *Phys. Rev. Lett.* **69**, 1524 (1992).
- [16] M. Farmigier and A. P. Gast, *J. Colloid Interface Sci.* **154**, 522 (1992).
- [17] R. Tao and Qi Jiang, *Phys. Rev. Lett.* **73**, 205 (1994).
- [18] K. C. Hass, *Phys. Rev. E* **47**, 3362 (1993).
- [19] J. Melrose, *Mol. Phys.* **76**, 635 (1992).
- [20] R. T. Bonnecaze and J. F. Brady, *J. Chem. Phys.* **96**, 2183 (1992).
- [21] J. Liu, T. Mou, Y. Zhu, E. Haddadian, J. Pousset, and S. Lim, in *Proceedings of the Fifth International Conference on ER Fluids, MR Suspensions, and Associated Technology* (Ref. [1]), p. 727.
- [22] T. C. Halsey and W. Toor, *J. Stat. Phys.* **61**, 1257 (1990); *J. Colloid Interface Sci.* **153**, 335 (1993).
- [23] Y. Zhu, E. Haddadian, T. Mou, M. W. Gross, and Jing Liu, *Phys. Rev. E* **53**, 1753 (1996).